

Characterizing urban infrastructural transitions for the Sustainable Development Goals using multi-temporal land, population, and nighttime light data

Eleanor C. Stokes^{a,b,*}, Karen C. Seto^b

^a NASA Goddard Space Flight Center, 8800 Greenbelt Rd, Greenbelt, MD, 20771, USA

^b Yale University, 380 Edwards Street, New Haven, CT, 06511, USA

ARTICLE INFO

Keywords:

Electrification
Informal settlements
Slums
Nighttime lights

ABSTRACT

Though urbanization is often linked to development gains, some regions in Asia, Latin America, and Sub-Saharan Africa have grown in urban population, while remaining bereft of basic services like reliable electricity. Daytime optical remote sensing has tracked urban land cover change for decades, but there have been few studies that have monitored whether infrastructure is keeping pace with demographic and land transitions. Here, we explore how fusing multi-temporal population and land data with nighttime lights data, derived from the Suomi-NPP VIIRS Day Night Band, can add to our understanding of urban infrastructural transitions. We classify urban changes in India and the US, using these three measures in tandem to create a typology of urban development processes. When compared against survey data, our results indicate the classification can track rural electrification and identify growing informal settlements with inadequate infrastructure, and is therefore useful for monitoring progress towards two Sustainable Development Goals: Goal 7.1 (ensure universal access to affordable, reliable and modern energy services) and Goal 11.1 (ensure access for all to adequate, safe and affordable housing and basic services and upgrade slums). The classification results also illustrate the diversity of urban development processes, and how uni-dimensional measures of urbanization, greatly under-represent urban change, particularly in high-income countries.

1. Introduction

Urbanization, at its core, is motivated by the search for a better life. For 10,000 years, humans have moved to cities, in part, to access social and economic opportunities and to escape rural poverty. This motivation continues to be a main driver of urbanization in the 21st century. In India, 300 million new urban residents are projected from 2016 to 2050 (UN-HABITAT, 2016), approximately the current population of the United States. Many of these new residents will migrate to urban areas in hopes of capitalizing on economic growth to improve their standard of living (Lee, 1966; Harris and Todaro, 1970; Fay and Opal, 1999).

The urban areas these migrants will arrive in vary considerably, both in their current capacity to provide improved living standards and their development trajectories. In some urban areas, urban population growth has been accompanied by economic growth, business, investments, increased revenues, and subsequent advancements in infrastructure services and human well-being. In other urban areas, urban

population growth has increased pressure on infrastructure that is already insufficient, under-funded, and under-developed (Brückner, 2012; Fox, 2012), leaving communities without the basic services necessary to live healthy lives. Cities in low and low-middle income countries have experienced the expansion of slums, widening inequalities, and lags in development as a by-product of their growing populations (Montgomery et al., 2013; Ravallion et al., 2007). Currently, 24% of India's urban population lives in informal settlements, without access to basic infrastructure services, like electricity (UN-HABITAT, 2017).

The divergent development trajectories of urban settlements have great importance to the quality of life of their residents (Amis and Kumar, 2000), human health (Satterthwaite, 2009; Boadi et al., 2005), and sustained economic growth (Turok and McGranahan, 2013). Understanding these trajectories is a key focus of multiple UN Sustainable Development goals (SDGs) and targets. In particular, targets 7.1 and 11.1 center on addressing the infrastructural challenges of urbanization—aiming to reduce the population living in areas with inadequate

* Corresponding author. Yale University, 380 Edwards Street, New Haven, CT, 06511, USA.

E-mail address: eleanor.stokes@nasa.gov (E.C. Stokes).

<https://doi.org/10.1016/j.rse.2019.111430>

Received 15 November 2018; Received in revised form 23 June 2019; Accepted 17 September 2019

Available online 23 October 2019

0034-4257/ © 2019 Elsevier Inc. All rights reserved.

infrastructural investment. Target 7.1 aims to ensure universal access to electricity, focusing mostly on electrification, while target 11.1 focuses on bolstering infrastructure inside urban areas, and upgrading slums. Both targets explicitly devote attention to energy services as one of the primary infrastructural needs of the inhabitants of developing settlements.

These targets require new ways of conceptualizing and monitoring urbanization, defining it not only as a demographic transition, but also as an infrastructural transition, a departure from how urbanization is predominantly characterized. Currently, urbanization is most often either monitored strictly as the percentage of the population residing in urban areas (e.g. by UN population projections (World Urbanization, 2014)), or as land change process by remote sensing. Though population growth and urban land expansion are important for understanding a myriad of environmental and social processes, neither directly link to quality of life improvements for urban residents. In contrast, growth in access to infrastructure services is central to human well-being—improving health, education, and income for the residents who benefit (Ramaswami et al., 2016; Parikh et al., 2015; Kanagawa and Nakata, 2008), and is a key focus of the SDGs. During this era of unprecedented urbanization, science and policy communities like those involved in UN-SDG bench-marking, require information about how well infrastructure advancements and access to basic services are paralleling urban population and land transitions. This information is critical for tracking development progress and guiding future investment.

Satellite images of the earth at night, which capture nighttime lighting (NTL) in urban areas, offer an opportunity to help close this information gap. By measuring increases in NTL over time, improvements in the availability of electricity to communities can be monitored. Use of nighttime data to study urban change is not new. NTL has been used extensively as a composite index of urbanization, where growth in NTL tracks some ambiguous combination of settlement expansion or densification, population growth, and infrastructural growth (Sutton et al., 2001; Sutton, 2003; Zhou et al., 2014; Ma et al., 2015; Zhang and Seto, 2011). Similarly, NTL have been applied in smaller urban settlements with the aim of tracking electrification, though distinguishing between electrification initiatives and settlement growth or redevelopment has required local knowledge (Min et al., 2013; Dugoua et al., 2018; Min and Gaba, 2014). This study is a departure from past work as it aims to disentangle infrastructure trends, from land and population trends, considering each of the three as independent transitions, that are all included under the umbrella term “urbanization”. Each dimension adds different information about “how” an area is being transformed, and taken together they can resolve a wider variety of urban development trajectories.

The goal of this re-conceptualization of urbanization is to identify areas with new investment, or insufficiency, in provision of basic services to residents. We aim to differentiate between urbanization where infrastructural development has kept pace with land and population changes versus where it has lagged behind. This paper explores the following questions: How ubiquitous is the predominant conception of urbanization—where infrastructure development occurs simultaneously with land change and population growth? Do satellite-derived infrastructure trends diverge from population, and land trends? If so, where and under what circumstances? How well do these divergences identify places with infrastructure deficits (e.g. slum development) as well as infrastructure initiatives (i.e. electrification)? By answering these questions, our methodology and results create relevant information for tracking the two aforementioned UN SDGs, and more broadly, for understanding the developmental trajectories of urbanization.

2. Prior uses of remote sensing to understand urban areas and urbanization

Remote sensing has played a central role in monitoring urbanization. Because Earth observation data is objectively measured, it

provides a means for consistent characterization of urban land and land change. There is a vast body of work that uses satellite data to map, measure, and quantify the amount of land taken up by human settlements (Mertes et al., 2015; Angel et al., 2011), contributing to our understanding of rates, magnitudes, and trajectories urbanization in different regions. Extensions of this research include the characterization of spatio-temporal patterns of urban land change (Herold et al., 2003; Deng et al., 2009; Song et al., 2016), which shape hydrology dynamics (Carlson and Arthur, 2000), climate (Kalnay and Cai, 2003), ecological studies (Grimm et al., 2008), biodiversity (Seto et al., 2012), and resource use (Foley et al., 2005).

Urban remote sensing has also focused on understanding the composition of urban land within urban areas. The classic V-I-S model, for example, uses the spectral reflectance of urban land surfaces to differentiate between vegetation, impervious surfaces, and bare soil, characterizing the physical geography within and between cities (Ridd, 1995; Wu and Murray, 2003). Recently, very high resolution (VHR) and SAR satellite data have been used as inputs into texture analyses to differentiate between neighborhood structures, and specifically to identify roof patterns associated with slums and informal housing (Duque et al., 2015; Wurm et al., 2017). This work has played an important role in illuminating the land morphology of urban areas, and in the case of slum-mapping, its associated social dimensions.

All of these previous studies monitor urban land and its built components, not the infrastructure services, such as electricity, used by urban residents. Contributions of remote sensing to understanding energy infrastructure are fewer, and primarily rely on NTL data.

Two satellite systems have collected NTL data. From 1970 until 2011, night imagery was collected solely by the Defense Meteorological Satellite Program (DMSP) using the Operational Linescan System (OLS). DMSP/OLS data has three well-documented disadvantages when it comes to studying urban areas and urbanization:

1. The spatial resolution of the DMSP/OLS is 2.7 km, which is often too coarse to characterize inter-urban variability.
2. The radiometric resolution of DMSP/OLS is constrained to 64 values (6 bits), resulting in saturated pixel values in urban centers.
3. Because of the lack of on-board calibration, radiometric quantities are not consistent across space or across time, rendering a time-series analysis difficult.

Despite these short-comings, DMSP/OLS NTL data has been used successfully to track urbanization dynamics in a similar manner to previous daytime studies—by identifying the quantity of land subsumed in regional urban growth (Liu et al., 2012; Zhou et al., 2015), as well as the timing, rate and spatial configuration of growth (Zhang and Seto, 2011, 2013; Gao et al., 2015; Ma et al., 2015; Pandey et al., 2013). When not a direct proxy for land area, NTL trends are treated as a composite measure in these studies, representing an aggregated, ill-defined mix of population, land, and economic change. To our knowledge, there are only a handful of nighttime remote sensing studies that have explicitly isolated changes in electricity access (Doll and Pachauri, 2010; Chand et al., 2009; Ramdani and Setiani, 2017), by considering NTL alongside population trends. However, because of DMSP/OLS's resolution and saturation effect, within-urban change is not a focus of these studies.

In 2011, the Visible Infrared Radiometer Suite Day Night Band (VIIRS-DNB), a new nightlights sensor, was launched into orbit on-board the satellite Suomi National Polar-orbiting Partnership Satellite (Suomi-NPP). VIIRS-DNB offers significant improvements to all three of the limitations that hindered the capability of DMSP/OLS in urban research:

1. VIIRS-DNB data has a 750 m spatial resolution, so each pixel is 13 times smaller in area than DMSP-OLS.
2. VIIRS-DNB also has a radiometric resolution of more than 65,000

values (16 bits), allowing it to detect variations in night light within the brightest urban centers, as well as amongst dark rural settlements.order

3. VIIRS has on-board calibration, capturing sensor data records that enable consistent measurement of radiances over time (Hillger et al., 2013).order

Along with these innovations in the sensor design, a multi-level processing algorithm that corrects for atmospheric scattering, fires, snow-cover reflectance, vegetation-occlusion, terrain-effects, and stray light has been recently developed, called Black Marble (Román et al., 2018). In the Black Marble algorithm, the lunar contribution to the VIIRS signal has also been removed, based on previous techniques for estimating the surface upward radiance from artificial nighttime light (NTL) sources (Cao et al., 2013; Walther et al., 2013; Johnson et al., 2013). The algorithm gap-fills cloud-covered pixels, and provides rigorous quality assurance and uncertainty information (Román et al., 2018). Compared to DMSP/OLS, the VIIRS-DNB archive is data-rich, since it is captured on a daily basis, and with Black Marble's corrections, all of the overpass dates can be used, instead of just the moon-free nights.

This study leverages the corrected Black Marble NTL as an independent estimator of energy infrastructure—a complement to urban population and land change. Our study focuses on two regions at different stages of urbanization: India, where rural to urban migration is rapidly underway, and the US, where urbanization is mature. India and the US are also good case studies because of the development disparities within and between the two countries (Human development i, 2018). The analysis includes all urban areas in India and the US, representing the entire continuum of tiny agricultural settlements to multi-million person metropolises.

3. Methods

Urbanization classes in the two countries are defined through a three-step methodology. First, we measure population, land, and infrastructure trends from 2012–2017. Our chosen time period of analysis is limited to the time period in which VIIRS NTL data is available. After measuring the trends, we use an unsupervised quantile clustering technique (Goswami and Chakrabarti, 2012) to assign geographical areas with similar combinations of population growth, land growth, and NTL growth to the same class. Finally, we use high-resolution Google Imagery to interpret the range of change processes and developmental trajectories captured in each class.

3.1. Measuring land, and infrastructure trends

3.1.1. Land cover trends

Global earth observation derived datasets have mapped the land associated with settlements for decades, but recently two new products have been made at a 10-fold increase in spatial resolution – Global Urban Footprint (GUF) (Esch et al., 2013), which relies on radar data from Tandem-X, and Global Human Settlement Layer (GHSL) (Pesaresi et al., 2013), which relies on optical data from Landsat. Since these datasets are new, there are few validation studies to assess their ability to capture settlements along the urban to rural continuum. Preliminary comparative assessments have found that these high-resolution settlement maps are more complete, precise, and accurate than their lower resolution counterparts, particularly for peri-urban and rural settlements (Klotz et al., 2016; Chowdhury et al., 2018), though some validation studies have highlighted omission errors in very sparse rural areas (Uhl et al., 2018; Mück et al., 2017).

To estimate the change in land cover, we use the Global Human Settlement Layer Degree of Built-up Area grid (GHSL Beta) (Pesaresi et al., 2016), because it is the only high resolution settlement map with historical layers available across multiple years. In this dataset, 38 m

binary land cover maps derived from Landsat that indicate the presence or absence of built up structures have been aggregated to a resolution of 300 m. During the aggregation, the estimated percent of built-up coverage (from the enclosed 38 m pixels) is assigned to each 300 m pixel as a raster value on a scale from 0–255, with 0 representing no built-up area and 255 representing total coverage (Pesaresi et al., 2013, 2016). We reprojected and resampled the GHSL data to 1 km so that it would match our other datasets, by averaging all pixels within the 1 km grid cells. GHSL data from 2000 and 2014 were used to evaluate the trend in built-up area change, and interpolated to match the 2012 to 2017 analysis dates.

3.1.2. Population trends

Two different datasets were used to track population change in the US and India. For India, we used the India v.2 dataset from WorldPop, a high resolution (100 m) open access population density raster, based on level 3 administration population estimates in the Indian census (Stevens et al., 2015), the most disaggregated level available publicly. WorldPop downscales population data using a random forest model based on 30 different variables, including both nighttime lights and land cover (Stevens et al., 2015), introducing some amount of endogeneity. The covariate importance of VIIRS-DNB and GHSL to the downscaling model, measured as a mean square error (%IncMSE), was approximately 35% and 22% respectively. This means that in rural areas in India, where level 3 census data is coarse, population distributions at the pixel level may be less reliable, reflecting the distribution of these covariates more than the actual population distribution. However, WorldPop does not use time series of these covariates as inputs. That is, for both 2010 and 2015 population estimates, a 2010 VIIRS-DNB composite and 2010 GHSL layer is used for spatial disaggregation. As a result population changes are independent of infrastructure and land changes, though they may be spatially misaligned.

Population estimates were provided by WorldPop for 2010, 2015, and 2020, with national totals adjusted to match UN population division estimates. We resampled the population rasters to 1 km resolution, to match the VIIRS-DNB imagery by computing the average of all non-“no data” contributing pixels. Linear trends of change between each of the three years (2010, 2015, 2020) were calculated, and 2012 and 2017 population estimates were created from these linear trends.

For the US, we used block level counts of population for 2010 (United States Census Bureau, 2010) and block group-level estimates of total population for 2014 from the American Community Survey, Table B01003 (United States Census Bureau, 2014), to create population density rasters. All of the rasters were first created at 100 m resolution, with the population density in each block and block group distributed equally over the administrative unit area. The rasters were then resampled to 1 km resolution using average resampling. As with India, the linear trend of change between 2010 and 2014 was calculated for each pixel, and population estimates for 2012 and 2017 were surmised from this linear model.

3.1.3. Infrastructure trends

To measure trends in electricity infrastructure development, we use daily nighttime top of atmosphere radiances over India and the continental United States from NASA's Suomi-NPP VIIRS-DNB (VNP46A1), archived at NASA's LAADS DAAC data center (<https://ladsweb.modaps.eosdis.nasa.gov/>). These data are then corrected for clouds, atmospheric, terrain, vegetation, snow, lunar, and stray light effects, using the Black Marble algorithm, described in detail in the algorithm theoretical basis document (ATBD) (Román et al., 2018). The corrected NTL data spans the time period from January 19, 2012 to September 30, 2017 for the continental US (2076 images) and from January 19, 2012 to September 13, 2017 for India (2057 images). The daily NTL data time-series for each pixel were smoothed using a 28 day rolling average to remove higher order noise, and spatially averaged on a 3x3 pixel moving window to address issues related to actual pixel coverage

within the VIIRS-DNB grid.

We produce a per-pixel time series trend line over the daily data, using a weighted least-squares linear regression model. Since each overpass of VIIRS does not provide an equally clear look at the earth, weighted least-squares linear regression is used because it allows each data point to have a different amount of influence over the regression model, depending on the data quality. Pixels with quality flag less than 2 (high quality and good-quality retrievals) are weighed at 100%, while quality flag 2 (poor quality retrievals) and quality flag 255 (no retrievals) are weighed at 20% and 0% respectively. We chose to weigh the poor quality retrievals at 20%, in order to minimize their influence on the regression model. Poor quality retrievals cannot be excluded altogether since some pixels have consecutive weeks without a good quality view (e.g. in the case of monsoon season in India). In these cases, the poor quality retrievals are still a better alternative than no value for these dates.

As a sensitivity check, STL decomposition was also performed on the time-series to remove any potential seasonal effects in the nightlights signal (Román and Stokes, 2015). We compared the STL decomposition trend slopes to the weighted least-squares linear regression trend slopes, but found that there was little difference in the results. Therefore, the linear regression was chosen because of its simplicity.

3.2. Quantile classification

To perform the classification, we first mask all of the areas in the US and India without built-up human settlements using a threshold GHSL<2. Since the GHSL degree of built-up coverage grid is a measure of how much of the pixel is covered by buildings, the threshold excludes areas where buildings make up less than 1% of the pixel coverage. This thresholding removes areas like farmland, wildland, and bare land. Pixels with more than 1% of their area covered by buildings are considered to be “settlement” pixels, inclusive of a broad rural village to dense metropolis gradient (Balk et al., 2019).

Next, we perform a classification on all the “settlement” pixels to cluster areas undergoing similar urbanization changes. One of the challenges of traditional unsupervised classifications in remote sensing is associating the resulting classes to their meaning. In order to bypass this use, we choose a quantile classification (Goswami and Chakrabarti, 2012), where the meaning of each class is defined a priori, since it is tied to the relative magnitude of each input variable. To perform the classification, we first take the absolute value of each trend slope for population, land cover, and NTL change, and standardize and normalize the trend slopes of each variable. The normalized trend slopes of each variable are then changed into quantiles, and divided into three groups (to represent low, medium, and high change). Finally, pixels with the same combination of population, land, and infrastructure change terciles are clustered together. For example, a pixel in the lowest tercile of population change, but the highest of NTL and land cover change would be in a different class than a pixel with the highest tercile of all three variables.

This classification yields 27 classes, since each variable has a high tercile, a medium tercile, and a low change tercile. Since the focus of this study is urbanization, we further filter the classification results to only include classes of “high” change for at least one variable—high population, infrastructure, or land change—during the time period of our study. This excludes pixels that are static or undergoing little change at all. Seven classes emerge—three with “high” change for only one variable, three with “high” change for two variables, and one with “high” change simultaneously for population, land cover, and NTL.

3.3. Ternary plot

We plot each of the pixels included in the classification on a ternary diagram to show their distribution amongst the seven urbanization classes. To find their position on the plot, we re-standardize the quantile

combinations of population, land, and NTL change such that the sum across the three variables is equal to 100%. For instance, a pixel with an equally high quantile of change for all three variables would occupy the center of the plot (33% infrastructure change, 33% land change, and 33% population change). One with only population growth would occupy the lower left corner.

3.4. Processing chain

The entire processing chain, including the resampling, spatial filtering, time-series smoothing, linear regressions, and quantile classification was performed using a combination of open source software libraries, including GDAL/OGRE (Development Team), Open Foris Geospatial Toolkit (Department, 2013), PKtools (Kempeneers, 2008), and Grass GIS (Development Team and G, 2012), and was run using Bash scripting on the Yale Omega Linux Cluster. The graphics were created with R (R Development Core Team, 2012) using the ggplot2 (Wickham, 2016) and ggtern packages (Hamiltonggtern, 2018).

4. Results

4.1. Typology of urbanization

To interpret the resulting classes, two-date time series Google earth images of a sample of 10 pixels (5 sample pixels from India and 5 from the US) within each of the seven urbanization classes are collected, totaling 140 images. The images are used to assess the assortment and most prevalent change processes represented by each class.

A typology of urbanization is created based on classification, that identifies seven distinct classes of urbanization (Fig. 1). They are described here, starting with the predominant conceptualization of urbanization, where simultaneously urban population increases, buildings are constructed on previously bare land, and electric infrastructure and other services are provided and propagated. We then describe departures from this type of simultaneous transition that were identified by the classification results. These include “independent” transitions,

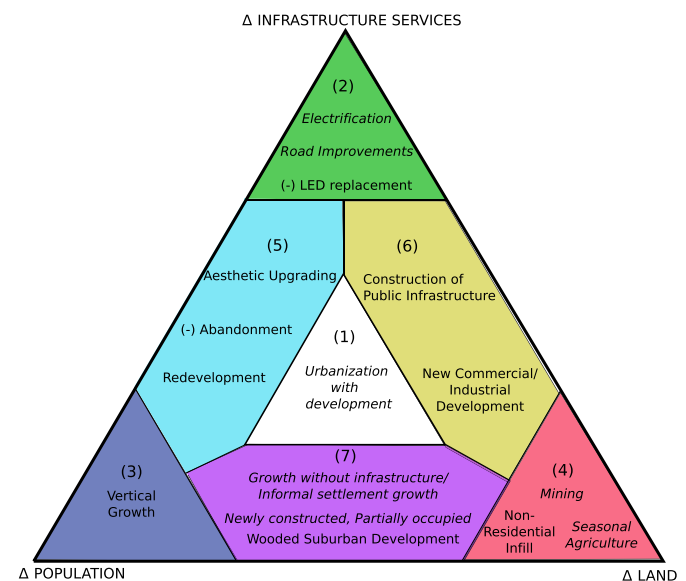


Fig. 1. Seven urbanization classes and examples of urban changes within each: (1) The center white triangle represents the common conceptualization of urbanization, concurrent change, where population, land cover, and infrastructure are simultaneously changing. The three corners of the ternary diagram represent independent transitions: (2) (de-)Electrification, (3) (de-)Densification, and (4) Land cultivation. Skewed transitions are represented by the three hexagons: (5) Redevelopment, (6) Non-residential development and (7) Dark growth.

where only one dimension (population, land cover, or electricity infrastructure) is changing, and “skewed” transitions, where only one dimension is not changing:

1. *Concurrent change* occurs when population, land, and electric infrastructure increase or decrease simultaneously, indicative of a concurrent demographic, structural, and developmental transition. *Concurrent change* is the type of development that is often imagined in reference to the term “urbanization”. This assumption is the basis for the use of NTL as a correlate of either population or land cover growth.

Independent transitions

2. *(de-)Electrification* occurs in regions that have stable land cover and population, but are under-going high electric infrastructure growth (or decline). The *electrification* class is directly related to SDG indicator 7.1.1, which monitors the proportion of population with access to electricity. From the samples collected, *electrification* occurred most commonly in rural and peri-urban areas of India, particularly in those targeted by government energy access initiatives and transportation corridor lighting development.

In contrast, the classification identified *de-electrification* within the center of urban areas in both the US and India, associated with decreases in NTL. This decrease in lighting was likely caused by LED streetlight installation, since the VIIRS-DNB sensor has no sensitivity below 400 nm, where LED lights peak. Validation of this hypothesis at a pixel level was not possible due to a lack of spatially and temporally-explicit urban lighting plans. However, national level statistics on LED proliferation are compelling. From 2012 to 2014, LED streetlights quadrupled in the US, growing from 3% to 13% of all roadway lighting (Yamada and Chwastyk, 2015). Similarly in India, the LED lighting market has risen at an annual growth rate of 40% over the past six years (Bonafide Research and India, 2017). In Indian cities, lamps in 3.5 million streetlights have been replaced with LEDs (Energy Efficiency Service, 2017).

3. *(de-)Densification* occurs in areas where population is growing (or decreasing) rapidly, while the land and infrastructure services are stable. This class commonly occurred in areas where the built environment was growing in the vertical dimension, without accompanied changes in the street grid or land uses. *Densification* may also occur without vertical growth, by increasing the number of residents per dwelling or building more space-efficient units.

4. *Land Cultivation* occurs when land cover is changing in isolation. Many of the areas labeled as *land cultivation* pixels were sites of interspersed seasonal agriculture within urban areas, mining, or other excavation industries. Sites of prospective development, where land clearing, or even the beginning states of construction, had occurred were also identified by this class.

Skewed transitions

5. *Redevelopment* includes regions where electricity infrastructure and population are simultaneously increasing or decreasing, but land is stable. *Redevelopment* with population and electric infrastructure growth, can be indicative of aesthetic upgrading and revitalization efforts. *Redevelopment* with population and electric infrastructure decline can indicate property abandonment and urban decay. Once built, urban buildings do not usually disappear, though they may be remodeled or reconfigured for other uses. As a result, population and light levels can decline, but land cover remains constant. The *redevelopment* class was most common inside the core of larger cities in the US and India.

6. *Non-residential Development* occurs when built-up land and electricity infrastructure are growing, but population numbers are constant or lag behind. Sampled pixels in this class were instances of urban land expansion in peri-urban areas, commercial or industrial development, or public project construction. For example, *non-residential development* captured the pattern of growth that characterized American “strip malls” and transportation corridor development, since these areas are often devoid of residents.

7. *Dark growth* is observed when population and land changes occur in tandem, without growth in electricity infrastructure services. In

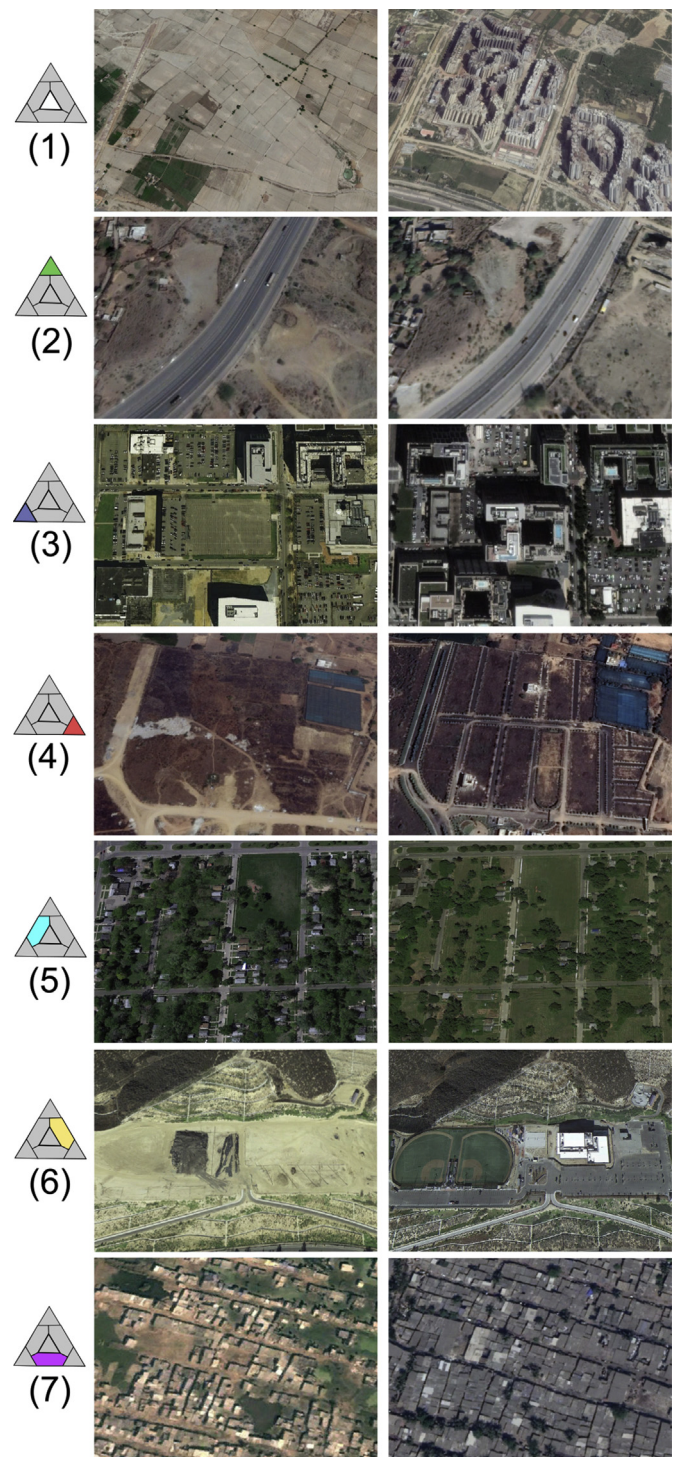


Fig. 2. Sample pixel sites of urbanization classes. Ternary diagrams in the top left corner indicate the type of urbanization in each site (Fig. 1): 1. Balaji Enclave residential apartment development in Noida, Uttar Pradesh (left) 2012, (right) 2017; 2. Road Electrification Project in Sethji Ki Kundal district of Udaipur. (left) 2013 without streetlights, (right) 2017 with streetlights; 3. Vertical Growth of apartments and redevelopment in Washington DC, (left) 2010 (right) 2017; 4. Land cover change from construction preparation in Hyderabad, India, (left) 2012, (right) 2017. 5. Land Abandonment in Brightmoor, Detroit, Michigan, where population decreased by 36% between 2000 and 2010. (left) 2010, (right) 2017; 6. Construction of new parking and public recreation infrastructure in Oak Park, California (left) 2012 (right) 2017; 7. Expansion and intensification of Navagaon informal settlement in Mumbai, India (left) 2006, (right) 2017.

India, this class was common in smaller towns, in regions where energy is less available. The class also identified growth in informal settlements where public lighting infrastructure was absent. In some areas of India, and most commonly in the US, *dark growth* occurred in suburban residential neighborhood development, where streetlights either were not installed or already existed before the construction of new neighborhoods. *Dark growth* relates to the measurement of SDG indicator 11.1.1, the proportion of urban population living in slums, informal settlements or inadequate housing. As the converse of *electrification*, dark growth does not directly measure the UN definition of a slum—areas “lacking one or more of the following conditions: access to improved water, access to improved sanitation, sufficient living area, and durability of housing.” However, electricity is a basic service, and if electricity infrastructure development is not keeping pace with population and settlement growth, investment in other basic services that are part of the slum definition (e.g. water, sanitation, and durable housing) may also be lacking.

Sample pixels from each class in the typology highlight the wide variety of urbanization and de-urbanization processes occurring in India and the US (Fig. 2). *Electrification* is observed in smaller villages in the north of India — e.g. Jharkhand, Uttar Pradesh, Bihar, Madhya Pradesh, and Haryana — and along newly developed primary and secondary transportation corridors. *Dark growth*, the opposite of *electrification*, was also prevalent in these northern states, indicating they are active areas for both current and future infrastructure investment.

The classification also identified pockets of *dark growth* within major Indian cities, like Kolkata and Mumbai (Fig. 2 F). These within-urban *dark growth* pixels corresponded to growing informal settlements and to large-scale periurban housing development projects, which were under construction and unoccupied. The misclassification of unoccupied housing developments as *dark growth* instead of *land cultivation* was an artifact of the low spatial resolution of the Indian population census. Because the administrative boundaries for publicly-available population data in India are coarse, there are errors in how population growth is downscaled and attributed to pixels, thus causing misclassification.

Dark growth is also apparent on the outskirts of US urban areas. In a high-income country context, *dark growth* occurred when suburban development was unaccompanied by additional lit street infrastructure, or the streetlight infrastructure was installed before 2012, when the VIIRS NTL record begins. Large swaths of *dark growth* suburban development are especially prevalent in peri-urban areas of the south-eastern US, because of the amount of land involved in new suburban development.

In contrast, the outskirts of major Indian urban areas, which fall most often in the *concurrent change* class, reflect India's less mature stage of urban development. Along with population and land change, new private developments outside of Indian urban cores have brought with them their own infrastructure and services. For example, residential projects in Delhi's satellite city, Noida (Fig. 2 (1)) have been the impetus for major street infrastructure projects, streetlight installations, brightly-lit malls, and all of the necessary civic infrastructure needed to attract international corporations and their employees. This development paradigm is unlike the US residential development, which is often built to rely on existing infrastructure and services.

4.2. Testing the validity of the urbanization typology for tracking SDG target 7.1

One of the proposed indicators for tracking SDG 7.1 (Ensure universal access to affordable, reliable, and modern energy services by 2030) is a measure of the proportion of the population with access to reliable electricity (Assembly, 2017). While the World Bank's Sustainable Energy for All (SE4All) Database (Foster et al., 2015) and the IEA World Energy Statistics and Balances (Agency, 2019) both provide country level data on grid-based electricity supply, local statistics are

rarely available to help identify the in-country distribution of deficits or to track the progress of targeted electrification initiatives. Furthermore, these databases do not include residents whose electricity access is supplied by off-grid and isolated mini-grid systems, which are increasingly common in remote areas both as both transitional and long-term power solutions (Bhattacharyya and Palit, 2016).

We test whether the results of the classification, and specifically the “electrification” class, can monitor electrification on a local level. In India, district level statistics on electrification are available from India's national electrification surveys. To test the validity of the classification, we compare the population living in class-derived *electrification* areas (corresponding to infrastructure development between 2012–2017) with these survey-based estimates collected by the government of India. We focus on rural settlements (the lower end of the urban gradient), because at the start of our study access to electricity was much lower in these settlements than in cities (56% of the rural population lacked electricity access vs 7% of the urban population (as defined by national statistical offices) in 2011 (Foster et al., 2015)).

We isolate “rural” *electrification* areas by excluding pixels that are more than 60% built up (corresponding to a GHSL threshold of 150 out of 255). The most common threshold for differentiating rural and urban areas is less inclusive, usually set at 50% built up area (Pesaresi and Freire, 2016; Balk et al., 2019). However, we chose to set a slightly higher threshold in order to avoid excluding larger villages and towns in agricultural regions, which have also been the target of energy infrastructure efforts in India.

We average the 2012 and 2017 residential population within rural *electrification* pixels for each Indian state to estimate the population that benefited from infrastructure investments, and compare these estimates to the number of Indian residents that gained electricity access between 2011 and 2016 from the national surveys. This number is derived by differencing the electrified population in the 2011 census (Indian Census Bureau and Sou, 2011) from that in the 2015–2016 National Family Health Survey (International Institute f, 2016) for each Indian state ($Population_{2016, state} - \%Elec_{2016, state} - Population_{2011, state} - \%Elec_{2011, state}$).

In performing this calculation, we make two assumptions that may affect the accuracy of the comparison. First, we assume that the whole population living in an *electrification* pixel benefits from electricity development, and that light increases in *redevelopment* or *concurrent change* pixels were not caused by electrification, but by structural modifications associated with population increases. Second, we assume that a change in the number of *electrification* pixels equates to a change in residential electricity access, though electrification of streetlights, railways, and public areas may not correspond to increased residential electricity services.

Our results (Fig. 3) show a weak, but positive linear relationship between census and class-based estimates. When all states are included, pixel-level electrification estimates explain 29% of the variation in the census-based electrification estimates ($R^2 = 0.289$). Delhi and Bihar are the two states with the highest deviance from the regression, due to many misclassified pixels. Delhi is a city state, consisting almost entirely of urban residents (97.5%). The edges of urban centers where urban infrastructure expansion projects, street light provision, LED-conversion, or road expansion have been abundant, were often classified as (*de*)-*electrification* pixels. The class-based estimate of Delhi's electrification labels all of these urban infrastructure transitions as electrification, and therefore estimates are higher than in surveys (violation of assumption 2). In contrast, Bihar is the most rural state in India, with almost 90% of the population living outside of urban areas. Whereas across India, rural population growth rates have declined between the last two censuses, Bihar witnessed the largest rural population growth rate at 24% (Indian Census Bureau and Sou, 2011). Since population increases are occurring alongside of infrastructure development, newly-electrified pixels are often classified as *redevelopment* in Bihar. Therefore, the class-based estimate of electrification is lower

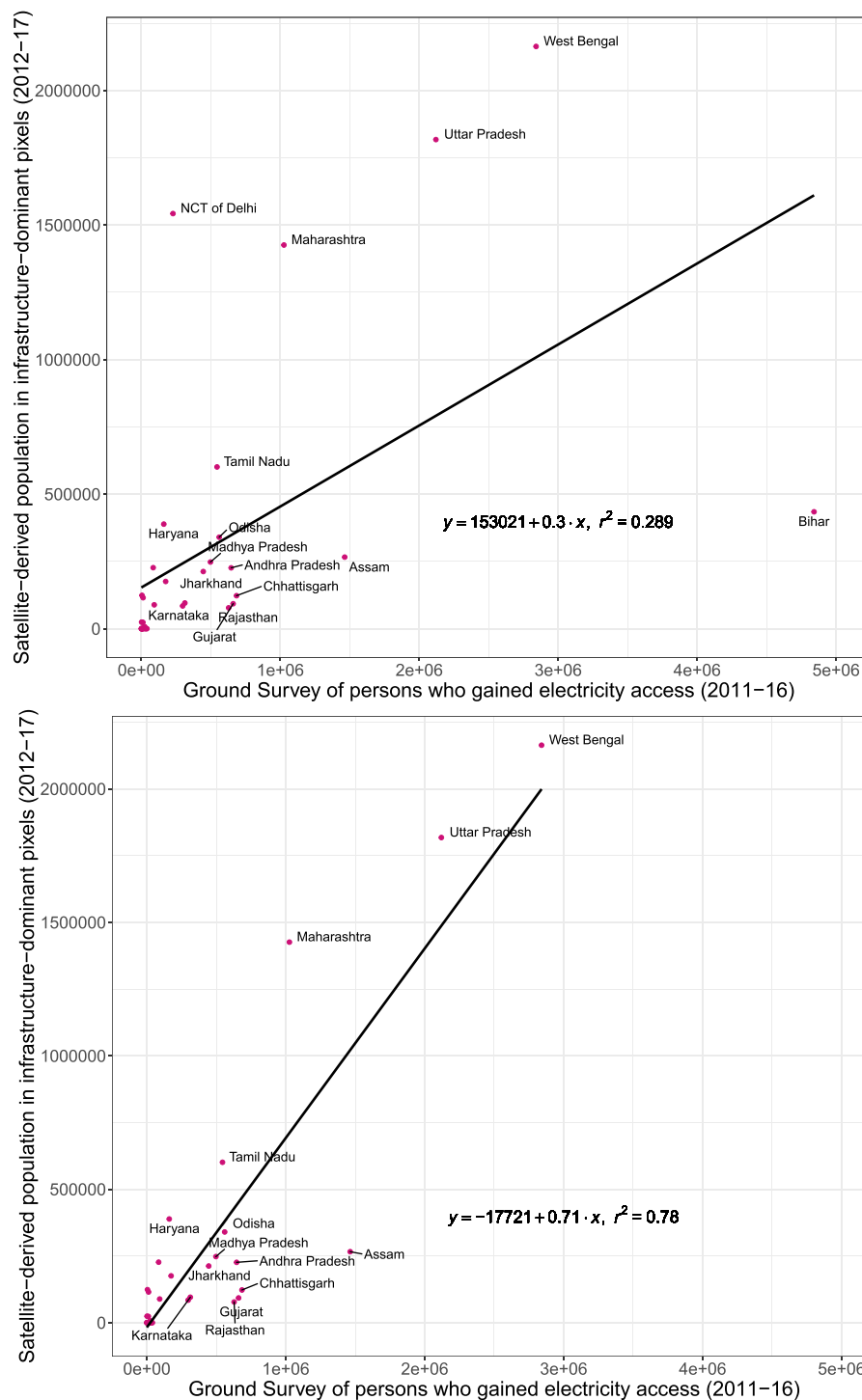


Fig. 3. Regression showing estimates of rural population gaining access to electricity between 2011 and 2017, based on the census and class-based estimates. (top) Regression including all Indian states (bottom) Regression excluding Delhi and Bihar.

than in surveys (violation of assumption 1). When both of these extremes– the most urban and most rural Indian state– are removed from the regression, the R^2 increased to .78.

The classification was particularly successful in detecting the large populations affected by rural electrification in Uttar Pradesh under the Deen Dayal Upadhyaya Gram Jyoti Yojana (DDUGJY) program and West Bengal under the Rajiv Gandhi Grameen Vidyutikaran Yojana (RGGVY) program, India's two previous flagship electrification schemes. In 2014, DDUGJY subsumed RGGVY, though both programs have worked toward connecting all villages in India to modern energy

services. The central government reports that 97,813 previously un-electrified villages in Uttar Pradesh were grid-connected under DDUGJY ([Indian Ministry of Power, 2018](#)), the highest of all Indian states.

4.3. Urbanization classes across India and the US

The classification highlights the variety of different development trajectories and urbanization processes, but how often do each of these urbanization processes occur? Are most “urbanizing” areas in India and

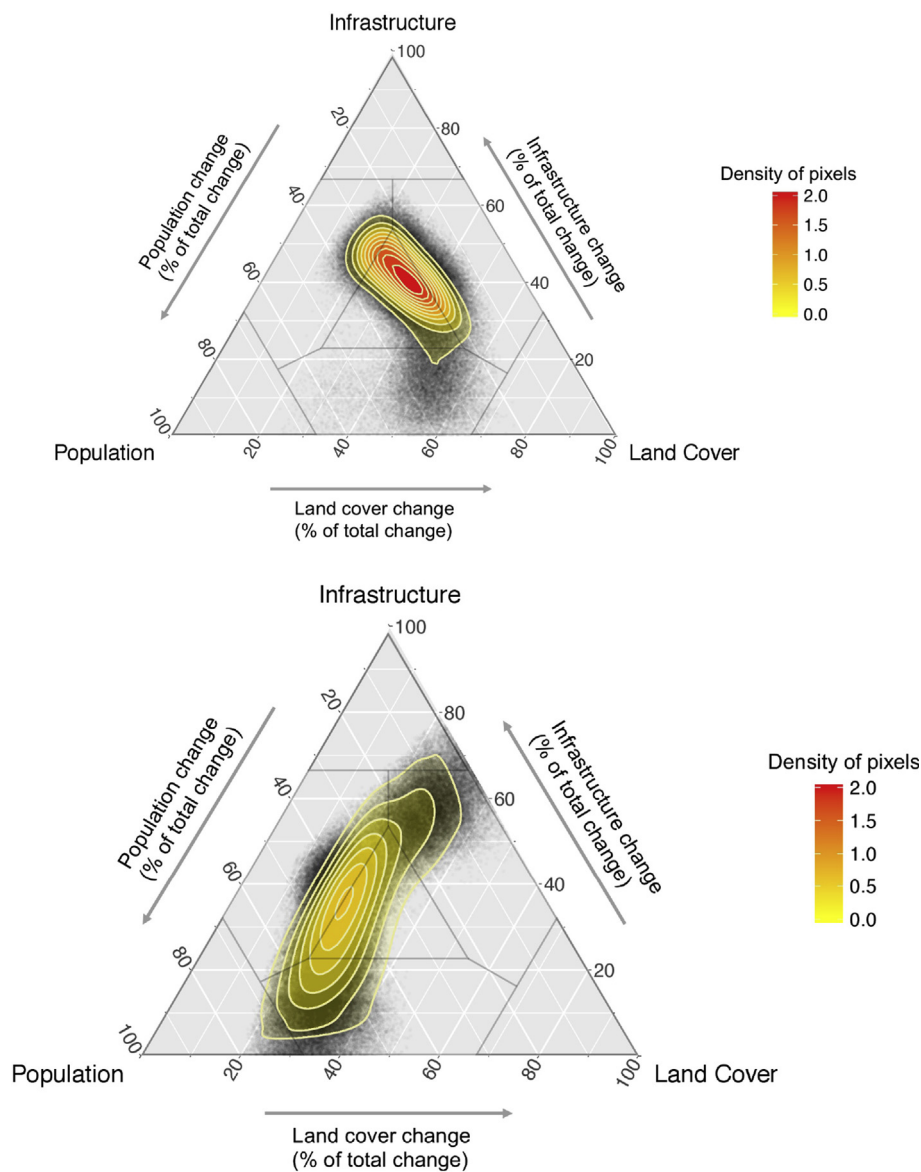


Fig. 4. Ternary diagram depicting the contribution of land, infrastructure, and population change to urbanization for each high-change pixel in India and the US (top) India, (bottom) US: Contour lines and the color gradient indicate different densities of pixels, determined by a 2-dimensional kernel density estimate, based on bivariate normal distributions. The density at a point is scaled so that the integral of density over all x and $y = 1$. (For interpretation of the references to color in this figure legend, the reader is referred to the Web version of this article.)

the US under-going *concurrent change*, as is most often assumed? How common is urbanization with infrastructural deficits (*dark growth*)?

We plot each of the pixels included in the classification on a ternary diagram (Fig. 4) to show their distribution amongst the urbanization types. A bivariate kernel density plot (Hamilton et al., 2018) is used with contour lines representing increases in the density of high change pixels. As shown, the results map the dominant classes of urbanization in the US and India (Fig. 4).

The epicenter of India's high change pixels—40% infrastructure change, 28% population change and 32% land change—shows that India's urbanization is dominated by electric infrastructure transitions. In contrast, the densest concentration of US change pixels consists of 35% infrastructure, 45% population, and 30% land change, dominated by population growth and decline. Urbanization in the Indian context populates the center and right side of the ternary diagram, signaling major land changes. Whereas, land change in the US context is more constrained, with few pixels deviating outside of the 15–40% range.

We find that Indian urbanization primarily consists of the *concurrent*

change class. The construction of large-scale new developments on previously agricultural or wild land involves simultaneous population, land, and electricity infrastructural transitions. This type of development is well-represented when using population datasets, NTL radiances, or built-up land area as parallel proxies. India's second largest urbanization classes are *redevelopment* and *non-residential development*, though both have far fewer pixels than concurrent change. The third largest class, *dark growth*, is represented as a less dense concentration of points at the bottom of the plot, with high land change (50%) high population growth (40%) but low infrastructure development (10%). The *dark growth* areas highlight energy availability constraints or a lag in public infrastructure development. These are important instances to map, since this is where urbanization is occurring without simultaneous development gains. Though we discuss the *electrification* class in the previous section, in terms of land area impacted, independent transition classes represent a very small proportion of the urbanization signal in India.

In contrast, US urbanization is more varied than Indian

urbanization, consisting of five classes: *commercial development*, *concurrent change*, *redevelopment*, *densification*, and *dark growth*. Because the US urbanization process is more mature, redevelopment and vertical growth on top of existing brownfields (*densification*) is common. For new greenfield development, we find all three typologies: strip development along major road corridors (*commercial development*), suburban development in peri-urban areas (*dark growth*), and *concurrent change* areas. As shown in the figure, urbanization in the US is as likely to be *redevelopment* as it is *concurrent change*.

5. Discussion and conclusion

Urbanization is one of the defining trends of the 21st century, shaping not only population dynamics and terrestrial systems, but also the development outcomes integral to human well-being. Urbanization can result in increased access to basic services, as in rural electrification, as well as increased inequalities and slum formation. The diverse development trajectories accompanying urbanization are not easily differentiated by daytime remote sensing datasets alone. With the implementation of the new UN Sustainable Development Goals, there is an urgent need to bring together data and develop methods that can explicitly capture improvements in access to modern energy services and other basic needs.

This study addresses this aim in three ways. First, the results are a considerable advancement over the status quo in how we conceptualize urbanization. It is well known that urbanization processes are varied, consisting of multiple (sometimes synchronous) transitions: transitions from dispersed to densely populated settlements, from natural and wild land to impervious built-up land, and from disconnected to modern and expansive infrastructure networks. Despite these varied processes, global and regional assessments have conceptualized urbanization monolithically, differentiating only between rates of urban population growth or land change, while leaving the character of change open to supposition. This study provides a new vocabulary and typology for discussing the wide variety of urbanization processes occurring across the globe in the 21st century. In particular, it creates urbanization classes where the implications for human welfare are explicit.

Second, the results both underscore the need, and offer a new methodology for how to measure urbanization so that is inclusive of a wider variety of urban change classes. If all urban change were *concurrent change*, multi-dimensional characterization would be redundant. However, our results show that much of the urban change in the US, and to a lesser degree in India is not *concurrent change*. In India, 17% of high change pixels were not *concurrent change* (where change from all three dimensions were balanced (all between 20% and 40% in the ternary diagram) (Fig. 1). In the US, 59% of the high change pixels were not *concurrent change*, meaning more than half of the urbanization signal could be overlooked by tracking urbanization with any singular variable. Therefore, uni-dimensional proxies greatly under-represent the quantity of urbanization occurring, particularly in the highest-income areas, where infrastructure and land transitions have already matured, and in the lowest-income areas, where infrastructural transitions are lagging behind. The method developed here expands the types of urban change detected. Population, land cover, and NTL are already collected globally, at high spatial and temporal resolution by satellite remote sensing and bottom-up demographic surveys. Their collection characteristics make them suitable input measures for defining urbanization classes that could be continuously monitored by national governments and custodian agencies of the UN Sustainable Goals.

Third, our results and methodology advance our understanding of how urbanization impacts sustainability, and particularly human development. The classes in the typology link urbanization to global change and sustainability issues of importance. For example, *concurrent change*, *commercial development*, and *dark growth* are all classes of urbanization that involve land cover changes. Urbanization that involves land changes has the potential to threaten biodiversity (Seto et al.,

2012) or heighten agricultural land loss (d'Amour et al., 2017), especially when it occurs at the frontier between the urban area and surrounding wild and rural land. In contrast, *population-dominant* and *infrastructure-dominant* classes have minimal land impacts, but are associated with other environmental problems—e.g. growing emissions, light pollution from new electricity infrastructure (Gaston et al., 2012), or increased air pollution from intensified urban activities (Fenger, 2009).

Similarly, the created urbanization classes identify urban change processes that are critical to human well-being: electricity availability, infrastructure replacement and upgrading, and growth without infrastructure services. We demonstrate that the *infrastructure-dominant* class tracks electrification efforts in rural India (Fig. 3) that would otherwise be unidentifiable through population or land cover change alone. Likewise, *dark growth* classes can be differentiated from *concurrent change*. These new capabilities in monitoring help development researchers and practitioners, track progress and target resources to the areas that need them most.

Despite these advancements, there are some limitations of the methodology employed in this study and challenges that remain before similar classifications could be used effectively to monitor rural electrification (SDG Goal 7.1) or the expansion of informal settlements (SDG Goal 11.1). The first is the difficulty of accuracy assessments of the classification. The types of processes examined (e.g. the installation of street lights, the vertical growth of buildings, slum development) can be difficult to ascertain via remotely sensed data, even when images are available. Comparing the classification results with ground-based surveys of electrification or informal settlement expansion was also difficult, due to a paucity of ground-collected data available at a high spatial resolution that matched the time period under investigation.

A second related challenge is the difficulty in interpreting the NTL trends. The use of VIIRS to study urbanization is complicated by a newly shifting electric lighting landscape, in both US and Indian cities. In 2010, LEDs had a less than 1% share of the solid-state lighting market in both OECD and non-OECD countries (Ashe et al., 2010; Bardsley et al., 2014). By 2030, OECD countries are expected to have a 50% share of LED luminaires in the commercial and industrial sector, and a 40% share of LED lamps in the residential sector (Bergesen et al., 2016; Baumgartner et al., 2012). The DNB sensor that collects Suomi-NPP's NTL data has no spectral sensitivity below 500 nm, which excludes a large portion of the typical LED spectral power distribution. The LED lighting transition in both India and the US poses a challenge for interpreting NTL time-series signals, especially within urban areas. Though the sensor sensitivity is a known quantity, no study has yet measured the sensitivity of trends in NTL to a massive LED transition in the electric lighting sector.

Finally, for inter-country assessments, the classification results were consistent and meaningful and revealed new information about development that is not currently available. However, a limitation for global-level analyses is that urbanization classes are not comparable across different development contexts. For example, the *Dark Growth* class was found both in growing informal settlements inside India's most population dense cities as well as in suburban US communities. The variety of processes clumped inside each urbanization class makes careful interpretation necessary before conclusions can be made about the processes occurring on the ground. To this point, we do not propose this typology as a replacement of ground-based surveys of electrification and informal settlement growth in countries that have the means to conduct these surveys. Instead, the proposed remote sensing-based methodology can serve as a complement or substitute to ground-based surveys when ground-based data are less available.

Despite these limitations, we find that the introduction of the NTL time-series, alongside daytime land sensors and population censuses, can help illuminate important aspects about the character of urbanization. The ability to differentiate between urbanization with and without infrastructure development, in particular, is timely. Along with

India, currently one of the fastest urbanizing regions of the world is in Sub-Saharan Africa. Many African urban areas have insufficient infrastructure, creating a lack of urban mobility and basic services. More than one billion people in Africa currently lack access to electricity. The data and methods used here show great potential to be expanded over these new geographies of change, where other social and economic development data is sparse. Extensions of this work could offer a new way to identify priority areas for infrastructure investment, and to advance urbanization monitoring efforts to include aspects of growth directly related to human well-being.

Acknowledgements

We would like to thank Miguel Roman and the NASA Goddard Terrestrial Systems Lab for providing early testing of the Black Marble algorithm for this publication. This work was supported by the NASA Harriett G. Jenkins Graduate Fellowship Program under NRA NNH16ZHA001N, the Yale Institute for Biospheric Studies, and Yale School of Forestry and Environmental Studies. E.C.S. also received funding from NASA's Applied Sciences program, NASA's Earth Science Data and Information Systems (ESDIS) project, and the NASA's Terra/Aqua/Suomi-NPP program, which supported our project under the following RTOP grants: NNH16ZDA001N-GEO16-0055, NNH17ZDA001N-TASNPP17-0007."

Appendix A. Supplementary data

Supplementary data to this article can be found online at <https://doi.org/10.1016/j.rse.2019.111430>.

References

- Agency, I.E., 2019. World Energy Balances. Accessed on 04.26.2019.
- Amis, P., Kumar, S., 2000. Urban economic growth, infrastructure and poverty in India: lessons from visakhapatnam. *Environ. Urbanization* 12, 185–196.
- Angel, S., Parent, J., Civco, D.L., Blei, A., Potere, D., 2011. The dimensions of global urban expansion: estimates and projections for all countries, 2000–2050. *Prog. Plan.* 75, 53–107.
- Ashe, M., Chwastyk, D., de Monasterio, C., Gupta, M., Pegors, M., 2010. *US Lighting Market Characterization*. US Department of Energy, Office of Energy Efficiency and Renewable Energy, Washington DC.
- Assembly, U.G., 2017. Global Indicator Framework for the Sustainable Development Goals and Targets of the 2030 Agenda for Sustainable Development. Technical Report, A/RES/71/313, July 2017. Retrieved from.
- Balk, D., Montgomery, M.R., Engin, H., Lin, N., Major, E., Jones, B., 2019. Urbanization in India: population and urban classification grids for 2011. *Data* 4, 35.
- Bardsley, N., Bland, S., Pattison, L., Pattison, M., Stober, K., Welsh, F., Yamada, M., 2014. Solid-state Lighting Research and Development Multi-Year Program Plan. US Department of Energy.
- Baumgartner, T., Wunderlich, F., Jaunich, A., Sato, T., Bundy, G., Griefsmann, N., Kowalski, J., Burghardt, S., Hanebrink, J., 2012. *Lighting the Way: Perspectives on the Global Lighting Market*. Technical Report, McKinsey and Company.
- Bergesen, J.D., Tähkämö, L., Gibon, T., Suh, S., 2016. Potential long-term global environmental implications of efficient light-source technologies. *J. Ind. Ecol.* 20, 263–275.
- Bhattacharyya, S.C., Palit, D., 2016. Mini-grid based off-grid electrification to enhance electricity access in developing countries: what policies may be required? *Energy Policy* 94, 166–178.
- Boadi, K., Kuitunen, M., Raheem, K., Hanninen, K., 2005. Urbanisation without development: environmental and health implications in african cities. *Environ. Dev. Sustain.* 7, 465–500.
- Bonafide Research, 2017. India Led Lighting Market Overview. pp. 2016–2022.
- Brückner, M., 2012. Economic growth, size of the agricultural sector, and urbanization in africa. *J. Urban Econ.* 71, 26–36.
- Cao, C., Shao, X., Upreti, S., 2013. Detecting light outages after severe storms using the S-NPP/VIIRS day/night band radiances. *IEEE Geosci. Remote Sens. Lett.* 10, 1582–1586.
- Carlson, T.N., Arthur, S.T., 2000. The impact of land use—land cover changes due to urbanization on surface microclimate and hydrology: a satellite perspective. *Glob. Planet. Chang.* 25, 49–65.
- Chand, T.K., Badarinath, K., Elvidge, C., Tuttle, B., 2009. Spatial characterization of electrical power consumption patterns over India using temporal dmsp-ols night-time satellite data. *Int. J. Remote Sens.* 30, 647–661.
- Chowdhury, P.K.R., Bhaduri, B.L., McKee, J.J., 2018. Estimating urban areas: new insights from very high-resolution human settlement data. *Remote Sens. Appl.: Soc. Environ.* 10, 93–103.
- Deng, J.S., Wang, K., Hong, Y., Qi, J.G., 2009. Spatio-temporal dynamics and evolution of land use change and landscape pattern in response to rapid urbanization. *Landsc. Urban Plan.* 92, 187–198.
- Department, F.F., 2013. Open Foris Geospatial Toolkit.
- GDAL Development Team, GDAL - Geospatial Data Abstraction Library, Version x.x.x, Open Source Geospatial Foundation, 201x.
- Doll, C.N., Pachaui, S., 2010. Estimating rural populations without access to electricity in developing countries through night-time light satellite imagery. *Energy Policy* 38, 5661–5670.
- Dugoua, E., Kennedy, R., Urpelainen, J., 2018. Satellite data for the social sciences: measuring rural electrification with night-time lights. *Int. J. Remote Sens.* 39, 2690–2701.
- Duque, J.C., Patino, J.E., Ruiz, L.A., Pardo-Pascual, J.E., 2015. Measuring intra-urban poverty using land cover and texture metrics derived from remote sensing data. *Landsc. Urban Plan.* 135, 11–21.
- d'Amour, C.B., Reitsma, F., Baiocchi, G., Barthel, S., Güneralp, B., Erb, K.-H., Haberl, H., Creutzig, F., Seto, K.C., 2017. Future urban land expansion and implications for global croplands. *Proc. Natl. Acad. Sci.* 114, 8939–8944.
- Energy efficiency services limited, street lighting national programme (SNLP), technical report. Ministry of Power.
- Esch, T., Marconcini, M., Felber, A., Roth, A., Heldens, W., Huber, M., Schwinger, M., Taubenböck, H., Müller, A., Dech, S., 2013. Urban footprint processor—fully automated processing chain generating settlement masks from global data of the tandem-x mission. *IEEE Geosci. Remote Sens. Lett.* 10, 1617–1621.
- GRASS Development Team, 2012. Geographic Resources Analysis Support System (GRASS GIS) Software. Open Source Geospatial Foundation.
- Fay, M., Opal, C., 1999. Urbanization without Growth: a Not-So-Uncommon Phenomenon. The World Bank.
- Fenger, J., 2009. Air pollution in the last 50 years—from local to global. *Atmos. Environ.* 43, 13–22.
- Foley, J.A., DeFries, R., Asner, G.P., Barford, C., Bonan, G., Carpenter, S.R., Chapin, F.S., Coe, M.T., Daily, G.C., Gibbs, H.K., et al., 2005. Global consequences of land use. *Science* 309, 570–574.
- Foster, V., Azuela, G., Bazilian, M., Sinton, J., Banerjee, S., Wit, J.d., Ahmed, A., Portale, E., Angelou, N., Liu, J., 2015. Sustainable Energy for All 2015: Progress toward Sustainable Energy. The World Bank.
- Fox, S., 2012. Urbanization as a global historical process: theory and evidence from sub-saharan africa. *Popul. Dev. Rev.* 38, 285–310.
- Gao, B., Huang, Q., He, C., Ma, Q., 2015. Dynamics of urbanization levels in China from 1992 to 2012: perspective from dmsp/ols nighttime light data. *Remote Sens.* 7, 1721–1735.
- Gaston, K.J., Davies, T.W., Bennie, J., Hopkins, J., 2012. Reducing the ecological consequences of night-time light pollution: options and developments. *J. Appl. Ecol.* 49, 1256–1266.
- Goswami, S., Chakrabarti, A., 2012. Quartile Clustering: A Quartile Based Technique for Generating Meaningful Clusters. arXiv preprint arXiv:1203.4157.
- Grimm, N.B., Faeth, S.H., Golubiewski, N.E., Redman, C.L., Wu, J., Bai, X., Briggs, J.M., 2008. Global change and the ecology of cities. *Science* 319, 756–760.
- Hamilton, N., ggtern, 2018. An Extension to 'ggplot2', for the Creation of Ternary Diagrams. R Package version 2.2.3.
- Harris, J.R., Todaro, M.P., 1970. Migration, unemployment and development: a two-sector analysis. *The American economic review*, pp. 126–142.
- Herold, M., Goldstein, N.C., Clarke, K.C., 2003. The spatiotemporal form of urban growth: measurement, analysis and modeling. *Remote Sens. Environ.* 86, 286–302.
- Hillger, D., Kopp, T., Lee, T., Lindsey, D., Seaman, C., Miller, S., Solbrig, J., Kidder, S., Bachmeier, S., Jasmin, T., et al., 2013. First-light imagery from suomi npp viirs. *Bull. Am. Meteorol. Soc.* 94, 1019–1029.
- UNDP, 2018. Human Development Indicators and Indices: 2018 Statistical Update Team. Indian Census Bureau, 2011. Source Lighting Data Sheet.
- Indian Ministry of Power, 2018. Villages Electrified across the Country.
- International Institute for Population Sciences, 2016. Key Findings from the 2015-16 National Family Health Survey.
- Johnson, R.S., Zhang, J., Hyer, E.J., Miller, S.D., Reid, J.S., 2013. Preliminary investigations toward nighttime aerosol optical depth retrievals from the viirs day/night band. *Atmos. Meas. Tech.* 6, 1245–1255.
- Kalnay, E., Cai, M., 2003. Impact of urbanization and land-use change on climate. *Nature* 423, 528.
- Kanagawa, M., Nakata, T., 2008. Assessment of access to electricity and the socio-economic impacts in rural areas of developing countries. *Energy Policy* 36, 2016–2029.
- Kempeneers, P., 2008. Pktools: Open Source Toolkit for Geospatial Data. pp. 2013.
- Klotz, M., Kemper, T., Geiß, C., Esch, T., Taubenböck, H., 2016. How good is the map? a multi-scale cross-comparison framework for global settlement layers: evidence from central europe. *Remote Sens. Environ.* 178, 191–212.
- Lee, E.S., 1966. A theory of migration. *Demography* 3, 47–57.
- Liu, Z., He, C., Zhang, Q., Huang, Q., Yang, Y., 2012. Extracting the dynamics of urban expansion in China using dmsp-ols nighttime light data from 1992 to 2008. *Landsc. Urban Plan.* 106, 62–72.
- Ma, T., Zhou, Y., Zhou, C., Haynie, S., Pei, T., Xu, T., 2015. Night-time light derived estimation of spatio-temporal characteristics of urbanization dynamics using dmsp/ols satellite data. *Remote Sens. Environ.* 158, 453–464.
- Mertes, C.M., Schneider, A., Sulla-Menashe, D., Tatem, A., Tan, B., 2015. Detecting change in urban areas at continental scales with modis data. *Remote Sens. Environ.* 158, 331–347.
- Min, B., Gaba, K., 2014. Tracking electrification in vietnam using nighttime lights. *Remote Sens.* 6, 9511–9529.
- Min, B., Gaba, K.M., Sarr, O.F., Agalassou, A., 2013. Detection of rural electrification in

- africa using dmsp-ols night lights imagery. *Int. J. Remote Sens.* 34, 8118–8141.
- Montgomery, M.R., Stren, R., Cohen, B., Reed, H.E., 2013. *Cities Transformed: Demographic Change and its Implications in the Developing World*. Routledge.
- Mück, M., Klotz, M., Taubenböck, H., 2017. Validation of the dlr global urban footprint in rural areas: a case study for Burkina Faso. *Joint Urban Remote Sensing Event. JURSE*, IEEE, pp. 1–4.
- Pandey, B., Joshi, P., Seto, K.C., 2013. Monitoring urbanization dynamics in India using dmsp/ols night time lights and spot-vgt data. *Int. J. Appl. Earth Obs. Geoinf.* 23, 49–61.
- Parikh, P., Fu, K., Parikh, H., McRobie, A., George, G., 2015. Infrastructure provision, gender, and poverty in indian slums. *World Dev.* 66, 468–486.
- Pesaresi, M., Freire, S., 2016. Ghs Settlement Grid Following the Regio Model 2014 in Application to Ghsl Landsat and Ciesin Gpw V4-Multitemporal (1975-1990-2000-2015). *JRC Data Catalogue*.
- Pesaresi, M., Huadong, G., Blaes, X., Ehrlich, D., Ferri, S., Gueguen, L., Halkia, M., Kauffmann, M., Kemper, T., Lu, L., et al., 2013. A global human settlement layer from optical hr/vhr rs data: concept and first results. *IEEE J. Sel. Top. Appl. Earth Obs. Remote Sens.* 6, 2102–2131.
- Pesaresi, M., Ehrlich, D., Ferri, S., Florczyk, A., Freire, S., Halkia, M., Julea, A., Kemper, T., Soille, P., Syrris, V., 2016. Operating Procedure for the Production of the Global Human Settlement Layer from Landsat Data of the Epochs 1975, 1990, 2000, and 2014. *Publications Office of the European Union*, pp. 1–62.
- R Development Core Team, R., 2012. *A Language and Environment for Statistical Computing*. R Foundation for Statistical Computing, Vienna, Austria.
- Ramaswami, A., Russell, A.G., Culligan, P.J., Sharma, K.R., Kumar, E., 2016. Meta-principles for developing smart, sustainable, and healthy cities. *Science* 352, 940–943.
- Ramdani, F., Setiani, P., 2017. Multiscale assessment of progress of electrification in Indonesia based on brightness level derived from nighttime satellite imagery. *Environ. Monit. Assess.* 189, 249.
- Ravallion, M., Chen, S., Sangraula, P., 2007. New evidence on the urbanization of global poverty. *Popul. Dev. Rev.* 33, 667–701.
- Ridd, M.K., 1995. Exploring a vis (vegetation-impervious surface-soil) model for urban ecosystem analysis through remote sensing: comparative anatomy for cities. *Int. J. Remote Sens.* 16, 2165–2185.
- Román, M.O., Stokes, E.C., 2015. Holidays in lights: tracking cultural patterns in demand for energy services. *Earth's future* 3, 182–205.
- Román, M.O., Wang, Z., Sun, Q., Kalb, V., Miller, S.D., Molthan, A., Schultz, L., Bell, J., Stokes, E.C., Pandey, B., Seto, K.C., 2018. Nasa's black marble nighttime lights product suite. *Remote Sensing of Environment*, pp. 113–143.
- Satterthwaite, D., 2009. The implications of population growth and urbanization for climate change. *Environ. Urbanization* 21, 545–567.
- Seto, K.C., Güneralp, B., Hutyrá, L.R., 2012. Global forecasts of urban expansion to 2030 and direct impacts on biodiversity and carbon pools. *Proc. Natl. Acad. Sci.* 109, 16083–16088.
- Song, X.-P., Sexton, J.O., Huang, C., Channan, S., Townshend, J.R., 2016. Characterizing the magnitude, timing and duration of urban growth from time series of landsat-based estimates of impervious cover. *Remote Sens. Environ.* 175, 1–13.
- Stevens, F.R., Gaughan, A.E., Linard, C., Tatem, A.J., 2015. Disaggregating census data for population mapping using random forests with remotely-sensed and ancillary data. *PLoS One* 10, e0107042.
- Sutton, P.C., 2003. A scale-adjusted measure of “urban sprawl” using nighttime satellite imagery. *Remote Sens. Environ.* 86, 353–369.
- Sutton, P., Roberts, D., Elvidge, C., Baugh, K., 2001. Census from heaven: an estimate of the global human population using night-time satellite imagery. *Int. J. Remote Sens.* 22, 3061–3076.
- Turok, I., McGranahan, G., 2013. Urbanization and economic growth: the arguments and evidence for africa and asia. *Environ. Urbanization* 25, 465–482.
- Uhl, J.H., Zoraghein, H., Leyk, S., Balk, D., Corbane, C., Syrris, V., Florczyk, A.J., 2018. Exposing the urban continuum: implications and cross-comparison from an interdisciplinary perspective. *Int. J. Digital Earth* 1–23.
- UN-HABITAT, 2016. *World Cities Report 2016. Urbanization and Development. Emerging Futures*. UN Habitat. Google Scholar, Nairobi.
- UN-HABITAT, 2017. *United Nation's Millennium Development Goals Database*. The World Bank DataBank.
- United States Census Bureau/American FactFinder, 2014. *B1003 : Total Population: 2010 – 2014 American Community Survey*. U.S. Census Bureau's American Community Survey Office, Washington, DC. <http://factfinder2.census.gov>.
- United States Census Bureau, 2010. *Decennial Census*. <https://www2.census.gov/geo/tiger/TIGER2010BLKPOPHU/>.
- Walther, A., Heidinger, A.K., Miller, S., 2013. The expected performance of cloud optical and microphysical properties derived from suomi npp viirs day/night band lunar reflectance. *J. Geophys. Res.: Atmosphere* 118.
- Wickham, H., 2016. *ggplot2: Elegant Graphics for Data Analysis*. Springer-Verlag, New York.
- UNPD, 2014. *World Urbanization Prospects: the 2014 Revision*.
- Wu, C., Murray, A.T., 2003. Estimating impervious surface distribution by spectral mixture analysis. *Remote Sens. Environ.* 84, 493–505.
- Wurm, M., Taubenböck, H., Weigand, M., Schmitt, A., 2017. Slum mapping in polarimetric sar data using spatial features. *Remote Sens. Environ.* 194, 190–204.
- Yamada, M., Chwastyk, D., 2015. *Adoption of Light-Emitting Diodes in Common Lighting Applications*, Technical Report. Navigant Consulting, Suwanee, GA (United States).
- Zhang, Q., Seto, K.C., 2011. Mapping urbanization dynamics at regional and global scales using multi-temporal dmsp/ols nighttime light data. *Remote Sens. Environ.* 115, 2320–2329.
- Zhang, Q., Seto, K.C., 2013. Can night-time light data identify typologies of urbanization? a global assessment of successes and failures. *Remote Sens.* 5, 3476–3494.
- Zhou, Y., Smith, S.J., Elvidge, C.D., Zhao, K., Thomson, A., Imhoff, M., 2014. A cluster-based method to map urban area from dmsp/ols nightlights. *Remote Sens. Environ.* 147, 173–185.
- Zhou, N., Hubacek, K., Roberts, M., 2015. Analysis of spatial patterns of urban growth across south asia using dmsp-ols nighttime lights data. *Appl. Geogr.* 63, 292–303.